Electronic Supplementary Material (ESI) for ChemComm.

Supporting Information

for

Light-Induced Modification of Silver Nanoparticles with Functional Polymers

Lukas Stolzer, Ishtiaq Ahmed, Cesar Rodriguez-Emmenegger, Vanessa Trouillet, Pascal Bockstaller, Christopher Barner-Kowollik and Ljiljana Fruk**

Materials

Di-*tert*-butyl dicarbonate (97%, Sigma-Aldrich), 2,2′-(ethylenedioxy)bis(ethylamine) (98%, Sigma-Aldrich), benzotriazole-5-carboxylic acid (99%, Sigma-Aldrich), triethylene glycol (≥99%, Sigma-Aldrich), silver dispersion (20 nm particle size, 0.02 mg·mL^{-1} in aqueous buffer, contains sodium citrate as stabilizer, Sigma-Aldrich), dimethyl sulfoxide (DMSO, ≥99%, Sigma-Aldrich), tetrahydrofuran (THF, ≥99.70%, VWR), dichloromethane (DCM, ≥99.80%, VWR), 1-hydroxybenzotriazole hydrate (HOBt, ≥97%, Sigma Aldrich), *N*,*N*′-dicyclohexylcarbodiimide (DCC, 99%, Sigma-Aldrich), *N*-hydroxysuccinimide (NHS, 98%, Sigma-Aldrich), trifluoroacetic acid (TFA, ≥99,9%, Roth), 4-(dimethylamino)pyridine (DMAP, 99%, Sigma-Aldrich) O-(benzotriazol-1-yl)-*N,N,N′,N′*-tetramethyluronium hexafluorophosphate (HBTU, ≥98.0%, Sigma-Aldrich), *N,N*-diisopropylethylamine (DIPEA, 99.5%, Sigma-Aldrich), copper(I) bromide (99,999%, Sigma-Aldrich), 2,2'-bipyridyl (BiPy, ≥99%, Sigma-Aldrich), 2-(dimethylamino)ethyl methacrylate (98%, Sigma-Aldrich), and β-propiolactone (≥90%, Sigma-Aldrich) were used as received. Synthesis of 4-((2-formyl-3-methylphenoxy)methyl)benzoic acid[1] and ω–maleimido-polyethylene glycol (PEG-Mal)[2] were performed according to literature procedures.

Characterization

^{1}H NMR spectroscopy was performed using Bruker AM 250, Bruker AM 300 or Bruker AM 400 spectrometer at 250 MHz, 300 MHz or 400 MHz, respectively. Samples were dissolved in $CDCl_3$, DMSO-d^6 or in methanol-d^4. The δ-scale is referenced to tetramethylsilane as the internal standard.

UV- Vis spectra were obtained using VARY 300 Scan UV-Visible Spectrometer (Varian Inc., Germany).

XPS (X-ray spectroscopy) measurements were performed using a K-Alpha XPS spectrometer (ThermoFisher Scientific, East Grinstead, UK). All the samples were analyzed using a microfocused, monochromated Al Kα X-ray source (400 μm spot size). The kinetic energy of the electrons was measured by a 180° hemispherical energy analyzer operated in the constant analyzer energy mode (CAE) at 50 eV pass energy for elemental spectra. Data acquisition and processing using the Thermo Avantage software is described elsewhere.[3] The spectra were fitted with one or more Voigt profiles (BE uncertainty: + 0.2 eV). The analyzer transmission function, Scofield sensitivity factors,[4] and effective attenuation lengths (EALs) for photoelectrons were applied for quantification. EALs were calculated using the standard TPP-2M formalism.[5] All spectra were referenced to the C1s peak of hydrocarbon at 285.0 eV

binding energy, controlled by means of the well-known photoelectron peaks of metallic Cu, Ag, and Au, respectively.

Electrospray Ionization-Mass Spectrometry (ESI-MS) spectra were recorded on an LXQ Scientific spectrometer (ThermoFisher Scientific, East Grinstead, UK) equipped with an atmospheric pressure ionization source operating in the nebulizer assisted electrospray mode. The instrument was calibrated in the m/z range 195−1822 using a standard containing caffeine, Met-Arg-Phe-Ala acetate (MRFA) and a mixture of fluorinated phosphazenes (Ultramark 1621) (all from Aldrich). A constant spray voltage of 6 kV was used and nitrogen at a dimensionless sweep gas flow rate of 2 (approximately 3 $L \cdot min^{-1}$) and a dimensionless sheath gas flow rate of 5 (approximately 0.5 $L \cdot min^{-1}$) were applied. The capillary voltage, the tube lens offset voltage and the capillary temperature was set to 10 V, 70 V, and 300 °C respectively. The samples were dissolved with a concentration of 0.1 $mg \cdot mL^{-1}$ in a mixture of THF and MeOH (3:2) containing 100 μmol of sodium triflate and infused with a flow of 10 $\mu L \cdot min^{-1}$.

Transmission Electron Microscopy (TEM) images were obtained using a CM200-FEG microscope (Philips) operating at 200 kV. Further TEM imaging, HAADF-STEM and energy dispersive X-ray spectroscopy (EDXS) were done on the Titan^3 80-300 TEM microscope (FEI) operating at 80 kV.

Zeta potential measurements were obtained using Nano Zeta-Sizer (ZS Nano, Malvern).

Fast Atom Bombardment Mass Spectrometry (FAB-MS): the mass spectra were measured using Finnigan MAT90 mass spectrometer.

Syntheses

Synthesis of benzotriazole photoenol linker 3 (BTPE)

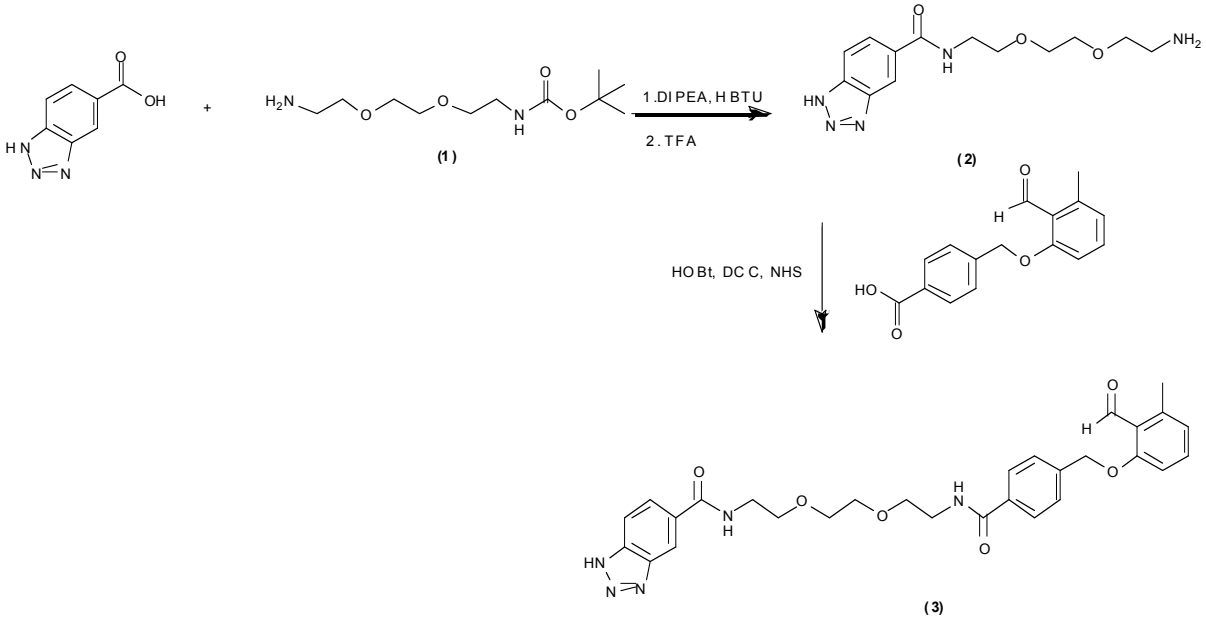

Scheme 1. Synthesis of N-(2-(2-(2-(4-((2-formyl-3-methylphenoxy)methyl)benzamido)ethoxy)ethoxy)ethyl)-1H-benzo[d][1,2,3]triazole-5-carboxamide **3** (BTPE).

Synthesis of *N*-Boc-2,2′-(ethylene-l,2-dioxy)bisethylamine (1)

Compound **1** was synthesized according to a reported method[6] with slight modification. A solution of di-*tert*-butyl dicarbonate (3.60 g, 16.8 mmol, 1 eq) in 60 mL CH_2Cl_2 was added to a solution of 2,2′-(ethylene-l,2-dioxy)bis(ethylamine) (5.00 g, 33.7 mmol, 2 eq) in 100 mL dry CH_2Cl_2 at 0 ^oC under argon atmosphere over a period of 6 h. The reaction mixture was stirred at 0 ^oC for 6 h and then at room temperature overnight. The solvent was removed under reduced pressure to afford light yellow residue which was dissolved in 50 mL of chloroform and washed twice with aqueous sodium bicarbonate solution. The combined organic layer was dried over anhydrous $MgSO_4$ and concentrated to give compound **1** (5.19 g, 20.96 mmol, 62%). ^1H NMR (300 MHz, $CDCl_3$) δ / ppm: 1.41 (s, 9 H, C*H*$_3$). 2.61 (t, *J* = 5.3 Hz, 2 H, C*H*$_2$), 3.02 (m, 2 H, C*H*$_2$), 3.24-3.36 (m, 4 H, C*H*$_2$), 3.38-3.44 (m, 4H, C*H*$_2$), 5.41 (br, 1 H, N*H*).

Synthesis of *tert*-butyl (2-(2-(2-(1*H*-benzo[*d*][1,2,3]triazole-5-carboxamido) ethoxy) ethoxy) ethyl) carbamate

To a solution of benzotriazole-5-carboxylic acid (1.00 g, 6.13 mmol, 1 eq) in dry THF/DMF mixture (8:2) (20 ml) was added HOBt (1.00 g, 7.36 mmol, 1.2 eq), HBTU (2.80 g, 7.36 mmol, 1.2 eq) and DIPEA (4.50 g, 18.4 mmol, 3 eq). The reaction mixture was cooled to 0 ^{o}C and *N*-Boc-2,2′-(ethylene-l,2-dioxy)bisethylamine **1** (1.67 g, 6.74 mmol, 1.1 eq) dissolved in THF (5 mL) was then added dropwise in 30 min. The slurry obtained was purged with argon and stirred overnight at room temperature. The volatiles were then removed under reduced pressure to obtain brown residue which was purified by silica gel chromatography starting with dichloromethane to dichloromethane/ methanol (20:1) to give a brown thick oil (1.87 g, 4.78 mmol, 78%).

^{1}H NMR ($CDCl_3$, 300 MHz) δ / ppm: 1.27 (s, 9 H, C*H*$_3$), 3.19 (t, *J* = 4.7 Hz, 2 H, C*H*$_2$), 3.45 (t, *J* = 4.9 Hz, 2 H, C*H*$_2$), 3.46-3.55 (m, 4 H, C*H*$_2$), 3.62-3.67 (m, 4 H, C*H*$_2$), 5.41 (m, 1 H, N*H*), 7.70 (d, *J* = 8.5 Hz, 1 H, H$_{Ar}$), 7.81 (d, *J* = 8.5 Hz, 1 H, H$_{Ar}$), 8.31 (s, 1 H, H$_{Ar}$); ^{13}C NMR ($CDCl_3$, 75 MHz): δ 28.5 (*C*H$_2$), 40.0 (*C*H$_2$), 40.2 (*C*H$_2$), 69.5 (*C*H$_2$), 69.9 (*C*H$_2$), 70.0 (*C*H$_2$), 79.3 (*C*(CH$_3$)$_3$), 114.1 (*C*$_{Ar}$), 115.5 (*C*$_{Ar}$), 125.1 (*C*$_{Ar}$), 131.7 (*C*$_{Ar}$), 139.4 (*C*$_{Ar}$), 156.3 (N*C*OO), 167.7 (O*C*N); FT-IR (ATR) ύ$_{max}$: 3325, 2976, 2927, 1690, 1643, 1542,1454, 1392, 1252, 1169 cm^{-1}; MS (+FAB): *m/z* (%): 394.2 (40) [M+H]$^{+}$, 338 (21), 294 (100), 189 (20), 154 (27); HR-MS: (FAB) *m/z* calculated for $C_{18}H_{28}N_5O_5$ [M + H]$^{+}$: 394.2094; found: 394.2090.

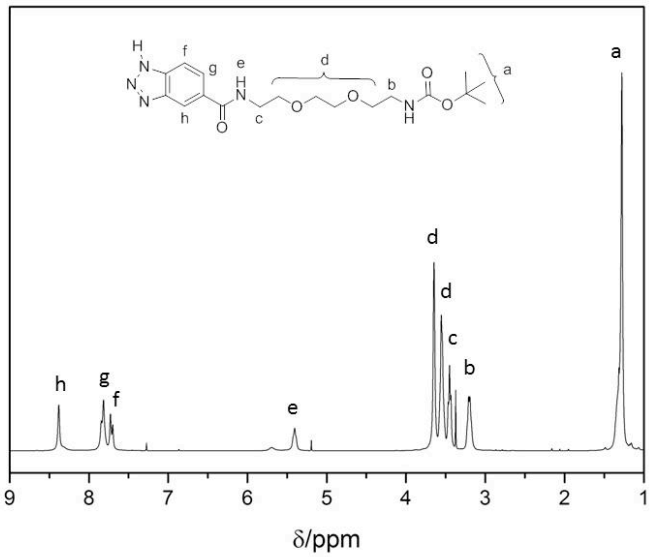

Figure S1. ^{1}H-NMR spectrum of *tert*-butyl (2-(2-(2-(1*H*-benzo[*d*][1,2,3]triazole-5-carboxamido)ethoxy)ethoxy)ethyl)carbamate in $CDCl_3$ at 300 MHz.

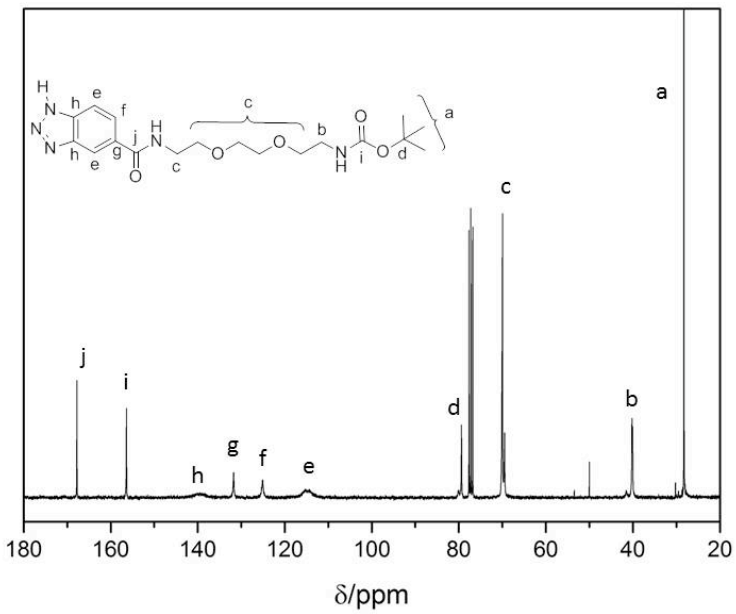

Figure S2. ^{13}C-NMR spectrum of *tert*-butyl (2-(2-(2-(1*H*-benzo[*d*][1,2,3]triazole-5-carboxamido)ethoxy)ethoxy)ethyl)carbamate in $CDCl_3$ at 300 MHz.

Synthesis of N-(2-(2-(2-aminoethoxy)ethoxy)ethyl)-1H-benzo[d] [1,2,3] triazole-5-carboxamide 2

To a stirred solution of *tert*-butyl (2-(2-(2-(1*H*-benzo[*d*][1,2,3]triazole-5-carboxamido)ethoxy)ethoxy)ethyl)carbamate (1.00 g, 2.54 mmol) in 15 mL dry CH_2Cl_2 was added TFA (6 mL). The reaction mixture was stirred at room temperature for 2 h. 15 mL CH_2Cl_2 was then added and the solvent was removed under reduced pressure. The procedure was repeated five times to remove traces of TFA to give compound **2** as brown oil in quantitative yield.

^{1}H-NMR (400 MHz, CD_3OD) δ / ppm: 2.99 (t, J = 5.1 Hz , 2 H, CH_2), 3.59-3.68 (m, 10 H, CH_2), 7.69 (d, J = 8.7 Hz , 1 H, H_{Ar}), 7.83 (d, J = 8.7 Hz , 1 H, H_{Ar}), 8.38 (s, 1H, H_{Ar}). ^{13}C- NMR (100 MHz, CD_3OD) δ / ppm: 40.87 (*C*H_2), 40.99 (*C*H_2), 69.40 (*C*H_2), 70.69 (*C*H_2), 71.33 (*C*H_2), 116.76 (C_{Ar}), 117.37 (C_{Ar}), 122.72 (C_{Ar}), 129.94 (C_{Ar}), 144.77 (C_{Ar}), 146.36 (C_{Ar}), 171.27 (O*C*N). HR-MS: (FAB) m/z calculated for $C_{13}H_{20}N_5O_3$ $[M + H]^+$, 294.1561; found, 294.1559.

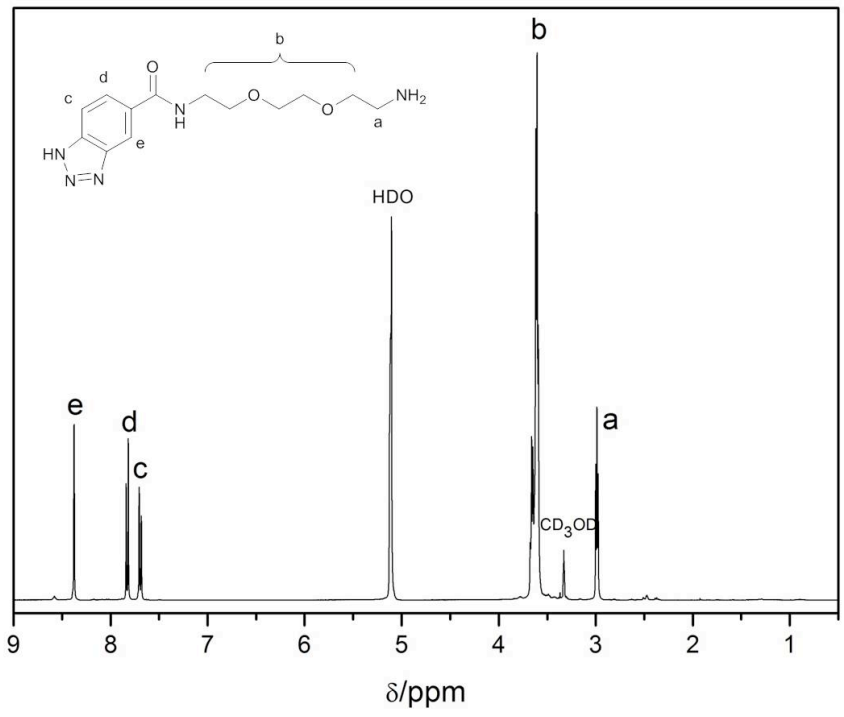

Figure S3. ^{1}H-NMR spectrum of *N*-(2-(2-(2-aminoethoxy)ethoxy)ethyl)-1H-benzo[d][1,2,3]triazole-5-carboxamide in CD_3OD at 400 MHz.

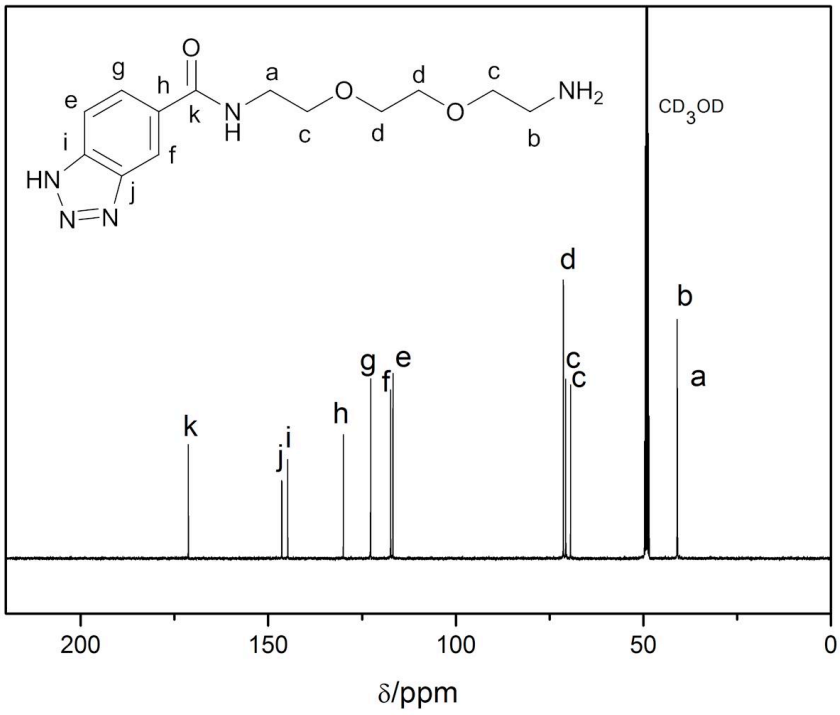

Figure S4. ^{13}C-NMR spectrum of N-(2-(2-(2-aminoethoxy)ethoxy)ethyl)-1H-benzo[d][1,2,3]triazole-5-carboxamide in CD_3OD at 100 MHz.

Synthesis of *N*-(2-(2-(2-(4-((2-formyl-3-methylphenoxy) methyl) benzamido) ethoxy) ethoxy)ethyl)-1H-benzo[d][1,2,3]triazole-5-carboxamide 3 (BTPE)

To bound 4-((2-formyl-3-methylphenoxy)methyl)benzoic acid to **2** as NHS ester, 73.0 mg (0.27 mmol, 1 eq) 4-((2-formyl-3-methylphenoxy)methyl)benzoic acid was dissolved in 1.5 mL of dry DMF. HOBt (37.0 mg, 0.28 mmol, 1.02 eq) was added and the solution was stirred for 10 min before addition of 61.0 mg (0.30 mmol, 1.1 eq) DCC (dissolved in 1.5 mL dry DMF). After stirring for 30 minutes, 32.0 mg (0.28 mmol, 1.02 eq) NHS dissolved in 1.5 mL dry DMF was added dropwise. The reaction mixture was stirred for 2 h. Compound **2** (80.0 mg, 0.27 mmol, 1 eq) dissolved in 1.5 mL dry DMF was added dropwise and the solution was stirred overnight. After filtration, the solvent was removed under reduced pressure and purified via column chromatography (chloroform/methanol 19:1) to obtain a white solid (50.0 mg, 0. 091 mmol, 34%).

^{1}H NMR (400 MHz, $CDCl_3$) δ / ppm: 2.45 (s, 3 H, C*H*$_3$), 3.58-3.61 (m, 12 H, C*H*$_2$), 5.00 (s, 2H, C*H*$_2$), 6.71 (t, *J* = 8.0 Hz, 2 H, C*H*), 7.20-7.29 (m, 3 H, C*H*), 7.41 (s, 1 H, C*H*), 7.57 (s, 1 H, C*H*), 7.71 (d, *J* = 8.2 Hz, 2 H, C*H*), 8,24 (s, 1 H, C*H*), 10.56 (s, 1 H, C*H*O). ^{13}C-NMR (100 MHz, $CDCl_3$) δ / ppm: 20.40 (*C*H$_3$), 38.97 (*C*H$_2$), 68.53 (*C*H$_2$), 68.66 (*C*H$_2$), 68.77

(CH_2), 69.16 (CH_2), 109.32 (C_{Ar}), 122.35 (C_{Ar}), 123.59 (C_{Ar}), 126.05 (C_{Ar}), 126.46 (C_{Ar}), 132.78 (C_{Ar}), 133.68 (C_{Ar}), 138.86 (C_{Ar}), 141.22 (C_{Ar}), 160.86 (C_{Ar}), 166.52 (O*C*N), 166.79 (O*C*N), 191.29 (*C*HO). HR-MS: (FAB) *m/z* calculated for $C_{29}H_{32}N_5O_6$ $[M + H]^+$, 546.2352 ; found, 546.2355.

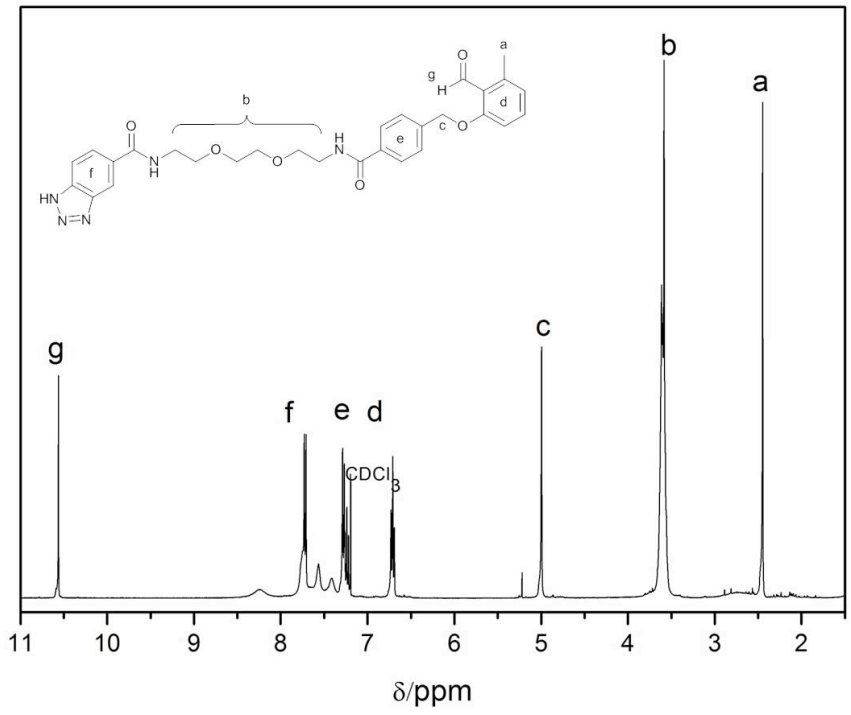

Figure S5. ^{1}H-NMR spectrum of BTPE **3** in $CDCl_3$ at 400 MHz.

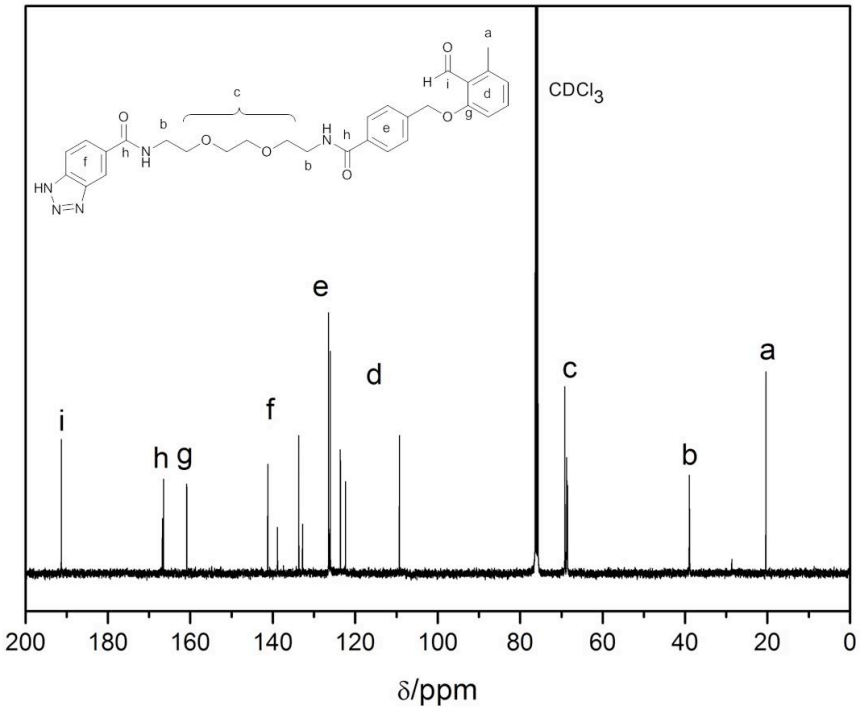

Figure S6. ^{13}C-NMR spectrum of BTPE **3** in $CDCl_3$ at 100 MHz.

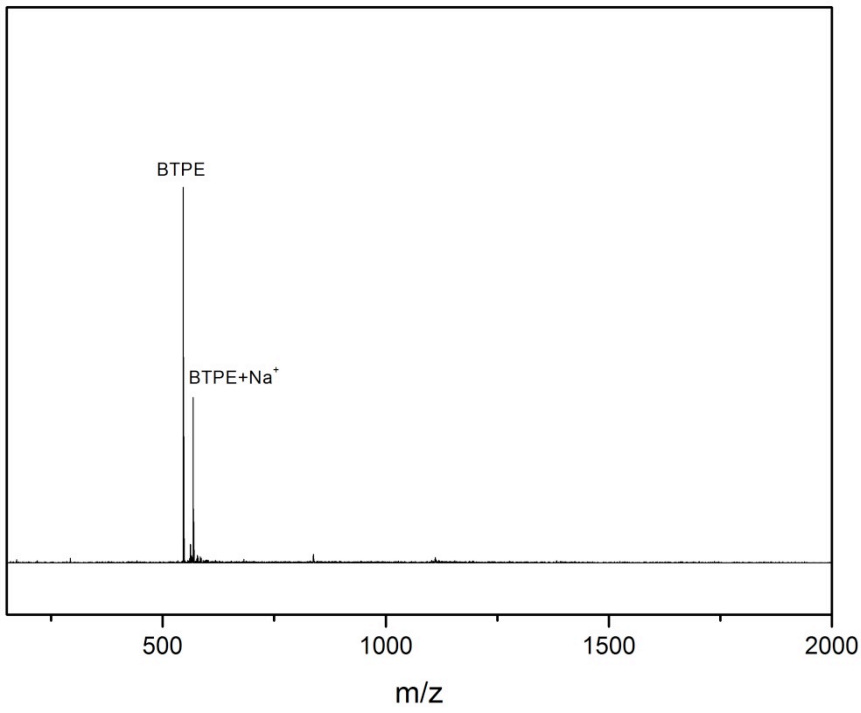

Figure S7. ESI-MS spectrum of BTPE **3**.

Synthesis of inert benzotriazole linker 4 (BTTEG)

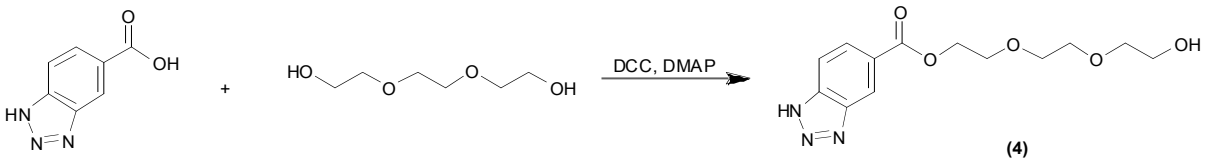

Scheme S2. Synthesis of 2-(2-(2-hydroxyethoxy)ethoxy)ethyl 1H-benzo[d][1,2,3]triazole-5-carboxylate **4** (BTTEG).

Synthesis of 2-(2-(2-hydroxyethoxy)ethoxy)ethyl 1H-benzo[d] [1,2,3] triazole-5-carboxylate 4 (BTTEG)

Benzotriazole-5-carboxylic acid (0,50 g, 3.07 mmol, 1 eq), triethylene glycol (TEG) (4.60 g, 30.7 mmol, 10 eq), DCC (0,76 g, 3.68 mmol, 1 eq), and DMAP (53.0 mg, 0.43 mmol, 0.14 eq) were dissolved in 20 mL THF and stirred under argon for 24 h at room temperature. The solvent was removed under reduced pressure and the crude product was purified via column chromatography (dichloromethane/methanol 9:1) to give **4** as yellow oil (0.52 g, 1.74 mmol, 57%).

^{1}H NMR (300 MHz, $CDCl_3$) δ / ppm: 3.68 (t, J = 4.4 Hz, 2 H, CH_2), 3.75-3.83 (m, 6 H, CH_2), 3.88 (t, J = 4.4 Hz, 2H, CH_2), 4.50 (t, J = 4.4 Hz, 2 H, CH_2), 7.76 (d, J = 8.7 Hz, 1 H, CH), 7.91 (d, J = 8.7 Hz, 1 H, CH), 8.53 (s, 1 H, CH). ^{13}C-NMR (75 MHz, $CDCl_3$) δ / ppm: 61.58 (*C*H_2), 64.23 (*C*H_2), 69.14 (*C*H_2), 70.22 (*C*H_2), 70.59 (*C*H_2), 72.52 (*C*H_2), 114.01 (C_{Ar}), 118.84 (C_{Ar}), 126.67 (C_{Ar}), 127.11 (C_{Ar}), 139.79 (C_{Ar}), 166.03 (O*C*O). HR-MS: (FAB) *m/z* calculated for $C_{13}H_{17}N_3O_5$ $[M + H]^+$, 295.1168 ; found, 295.1166.

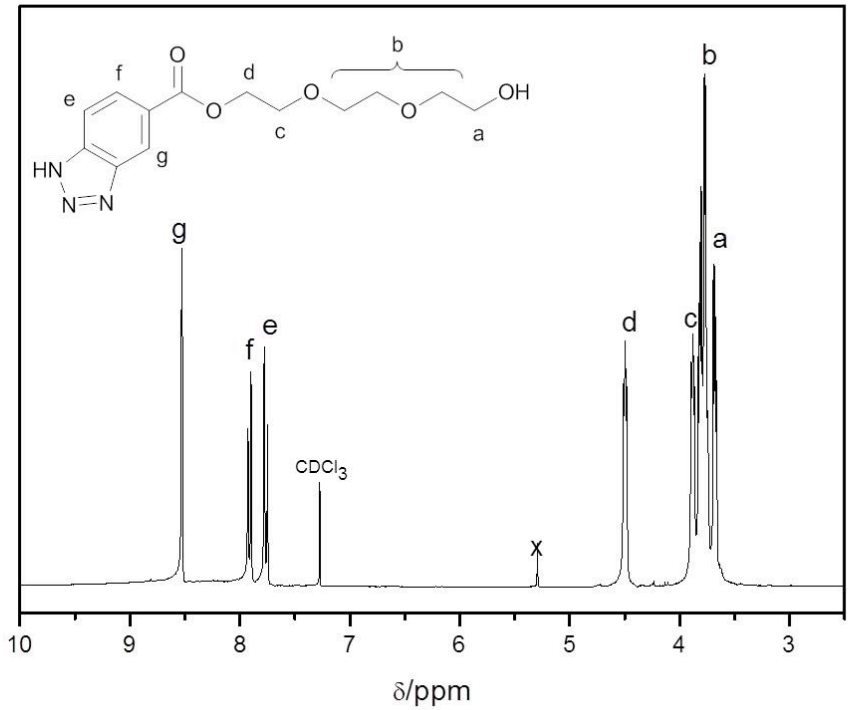

Figure S8. ^{1}H-NMR spectrum of BTTEG **4** $CDCl_3$ at 300 MHz.

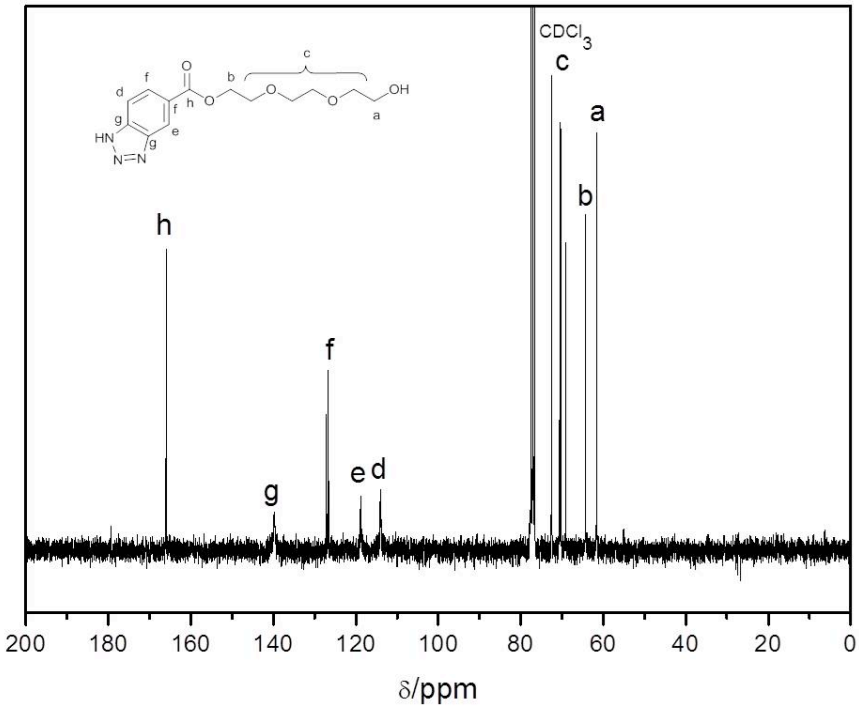

Figure S9. ^{13}C-NMR spectrum of BTTEG **4** in $CDCl_3$ at 75 MHz.

Initiator synthesis

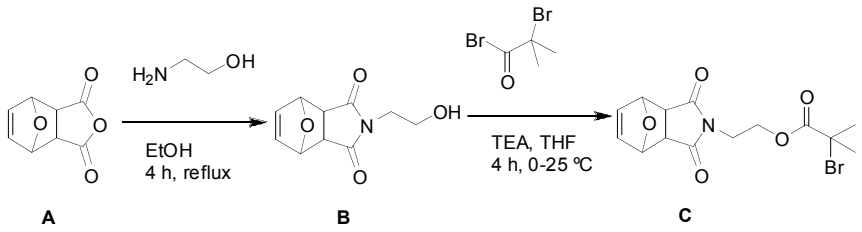

Scheme S3. Synthesis of 2-Bromo-2-methyl Propionic Acid 2-(3,5-Dioxo-10-oxa-4-aza-tricyclo[5.2.1.02,6]dec-8-en-4-yl) ethylester (C) (protected maleimide-initiator, **C**).

4-(2-Hydroxy-ethyl)-10-oxa-4-aza-tricyclo[5.2.1.0$^{2,6|}$dec-8-ene-3,5-dione (B)

Compound **B** was synthesized according to a previously reported procedure.[7] Furan **A** (50.0 g, 300 mmol, 1 eq) was suspended in 75 mL of EtOH and the mixture was cooled to 0 ºC. Subsequently, a solution of ethanolamine (18.8 mL, 300 mmol, 1 eq) in EtOH (15 mL) was added dropwise, and stirred for 10 min at 0 ºC, 30 min at ambient temperature and 4 h at reflux. The reaction mixture was allowed to cool down overnight and the crystalized product was filtrated. The obtained off-white crystals were dried under vacuum (Yield 44 %). ^{1}H-NMR spectroscopy (250 MHz, DMSO) δ / ppm: 6.55 (br, 2H, –CHC*H*=C*H*CH–), 5.12 (br, 2H, –C*H*CH=CHC*H*–), 4.79 (br, 1H, NCH$_2$CH$_2$O*H*), 3.41 (m, 4H, NC*H*$_2$C*H*$_2$OH), 2.93 (s, 2H, O=CC*H*).

2-Bromo-2-methyl PropionicAcid 2-(3,5-Dioxo-10-oxa-4-aza-tricyclo[5.2.1.0^{2,6}]dec-8-en-4-yl) ethylester (C)[8]

To a cooled solution (0 ºC) of the alcohol **B** (5.00 g, 23.9 mmol, 1 eq) and TEA (2.38 mL, 26.4 mmol, 1.1 eq) in 270 mL of dry THF, α-bromoisobutyryl bromide (3.15 mL, 25 mmol, 1.04 eq) in 90 mL of dry THF was added dropwise. The suspension was stirred for 3 h at 0 ºC and subsequently at ambient temperature overnight. TLC (SiO_2, ethyl acetate, R_f (**C**) = 0.42 and R_f (**B**) = 0.15) showed complete disappearance of the starting material **B**. The ammonium salt was filtered off and the solvent was evaporated under reduced pressure. The pale yellow liquid was further purified by flash chromatography (SiO_2, ethyl acetate:petroleum ether 1:1) to obtain a white solid. Yield (70 %).^{1}H NMR (250 MHz, $CDCl_3$) δ / ppm: 1.86 (s, 6H, CH_3), 2.84 (s, 2H, O=CC*H*), 3.78 (t, ^3J = 5.3 Hz, 2H, NC*H*$_2$), 4.30 (t, ^3J = 5.3 Hz, 2H, OC*H*$_2$), 5.23 (br, 2H, –C*H*CH=CHC*H*–), 6.49 (br, 2H, –CHC*H*=C*H*CH–).

Synthesis of carboxybetaine methacrylate (CBMA-2)

The title compound was synthesized by a modification of the procedure reported earlier (see Scheme 4).[9] *N,N*-dimethylaminoethyl methacrylate (15.7 g, 100 mmol) was dissolved in

120 mL of dry THF and cooled to 0 ºC. A small quantity of diphenylpicryl hydrazyl (DPPH) was added as inhibitor. Subsequently, β-propiolactone (11.0 g, 160 mmol) was dissolved in 50mL of dry THF and added dropwise under nitrogen for 3 h. The reaction was allowed to proceed for 24 h at 4 ºC. The white precipitate was filtered-off and subsequently washed with dry THF and ether. The product was dried under high vacuum. Prior to polymerization, DPPH was removed by reprecipitation into THF from methanol to yield 13.1 g (yield: 56%) of CBMA-2 as a white solid.

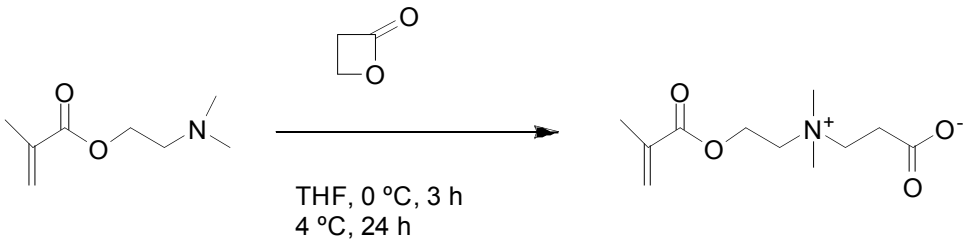

Scheme 4. Synthesis of carboxybetaine methacrylate (CBMA-2).

Polymerization of carboxybetaine methacrylate (poly(CBMA-2))

The polymerization of carboxybetaine methacrylate was carried out as a modification of our optimized procedures presented earlier.[10, 11] CBMA-2 (1.0 g, 4.4 mmol), protected maleimide initiator (120.0 mg, 0.225 mmol), 8 mL DMF and 4 mL water were added to a Schlenck tube. To a second Schlenck tube was added CuBr (32.0 mg, 0.225 mmol) and HMTETA (73 µL, 0.270 mmol), desoxygenated by cycling nitrogen and vacuum. To this tube 2 mL of DMF previously degassed was added. Both Schlenck tubes were subsequently degassed by 4 freeze-pump-thaw cycles. The catalyst solution (CuBr and HMTETA) were transferred using a gas-tight syringe to the Schlenck tube containing the monomer and initiator to start the polymerization. Polymerization was allowed to proceed for 24 h at room temperature to achieve 95% conversion. The polymer solution was dialyzed against water using a SpectraPor3 membrane (MW Cut-off 1000 g·mol^{-1}). Water was exchange thrice a day for 3 days. The freeze-dried polymer was characterized by absolute size SEC using an HPLC Shimadzu with a Superose 6 column equipped with UV, differential refractometer Optilab rEX and multiangle light scattering detector DAWN 8 (Wyatt Technology Corp., USA). 0.3 M sodium acetate buffer (pH 6.5) containing 0.5 g·L^{-1} sodium azide was used as the mobile phase. The poly(CBMA-2) displayed a M_n 21700 g·mol^{-1}.

The polymer was redissolved in toluene and refluxed for 6 h. The toluene was removed under reduced pressure, and the polymer was dried under high vacuum.

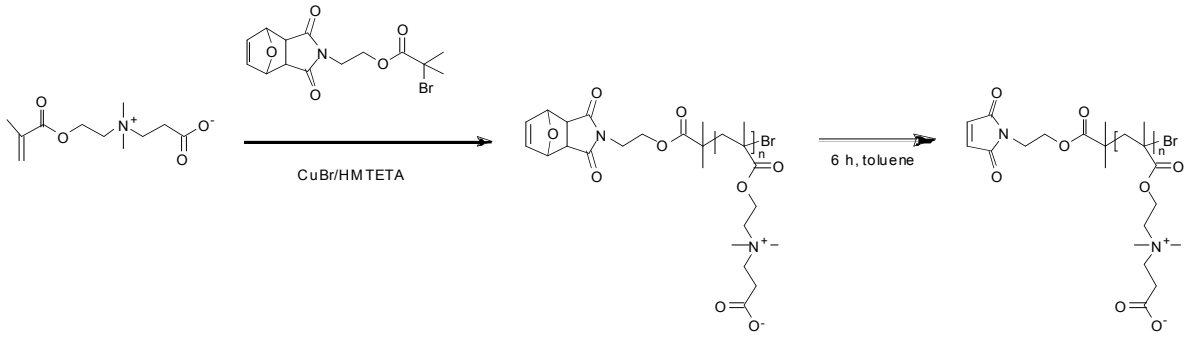

Scheme 5. Atom transfer radical polymerization (ATRP) of carboxybetaine methacrylate (CBMA-2) and deprotection of the maleimide group.

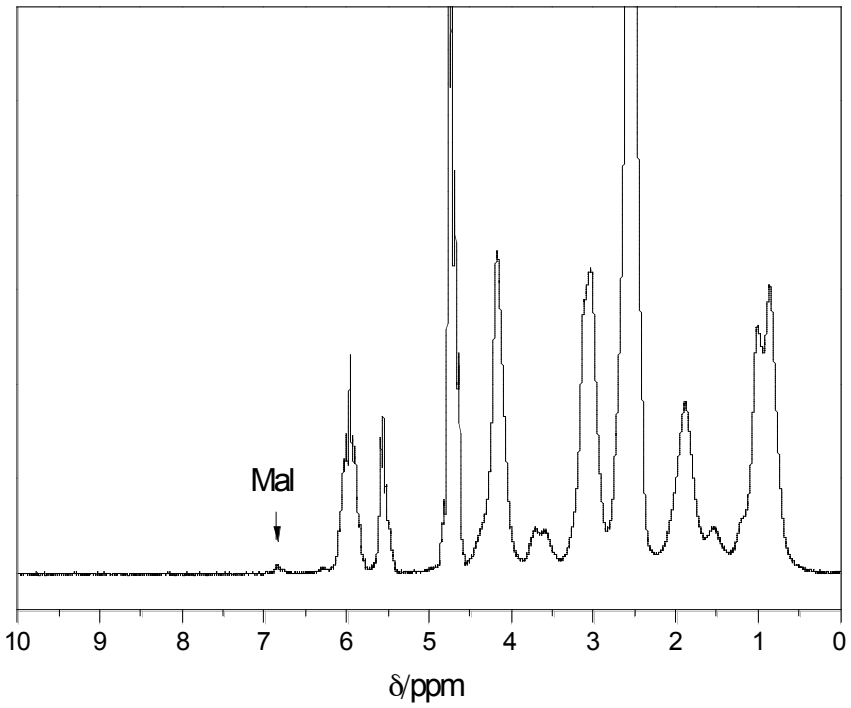

Figure S10. ^{1}H-NMR spectrum of poly(CBMA-2) in D_2O at 250 MHz.

Electrospray Ionization-Mass Spectrometry

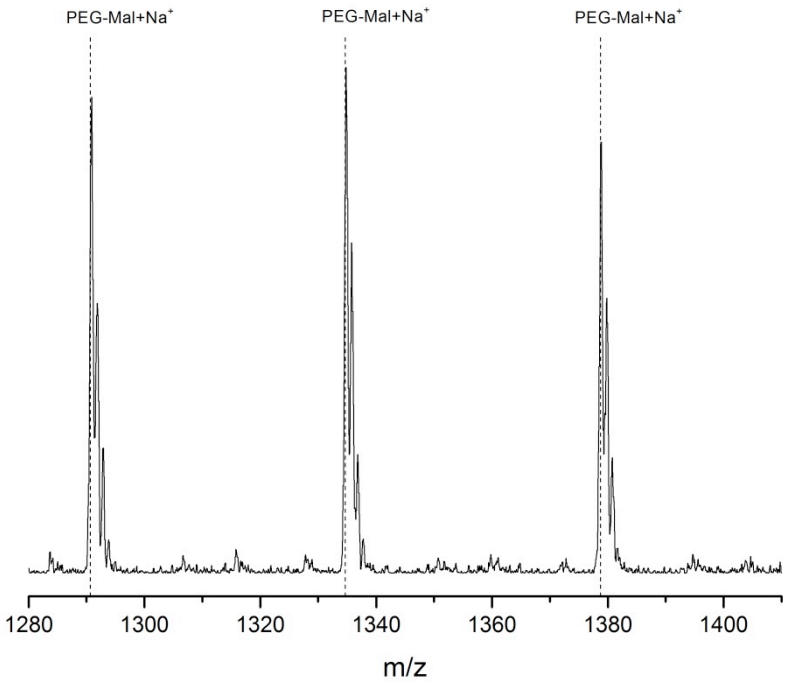

Figure S11. Zoom into the ESI-MS spectrum of PEG-Mal. The label indicates the theoretical mass of chains ionized with Na^+ (stemming from added NaTFA).

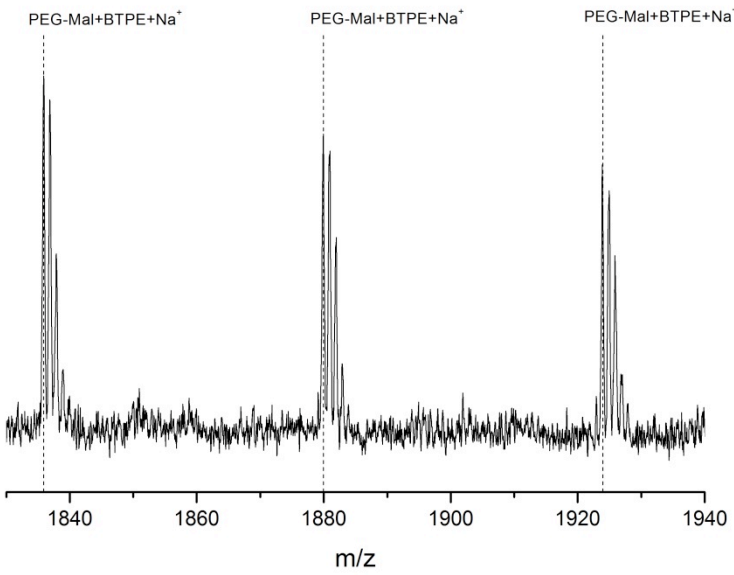

Figure S12. Zoom into the ESI-MS spectrum of the photoreaction between PEG-Mal and BTPE after 15 min irradiation. The label indicates the theoretical mass of chains ionized with Na^+ (stemming from added NaTFA).

Table S 1 Experimental and theoretical m/z values for the labelled peaks of **Figure S 11** and **Figure S12**.

m/z_{exp}	assignment	formula	m/z_{theo}	$\Delta m/z$
1334.77	PEG-Mal+Na	$[C_{59}H_{109}N\ O_{30}Na]^+$	1334.69	0.08
1879.92	PEG-Mal+ BTPE+Na	$[C_{88}H_{140}N_6\ O_{36}Na]^+$	1879.92	0.00

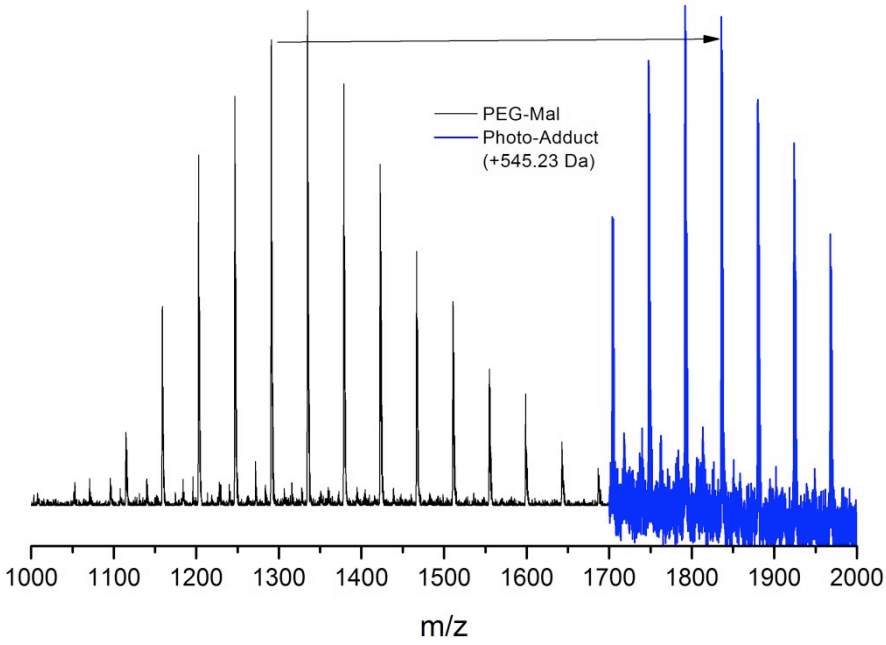

Figure S 13. Zoom into the single charged region of the ESI-MS spectrum of the model reaction between BTPE and PEG-Mal. The blue spectrum shows the photo-adduct after 15 min irradiation. The shift of the peaks matches the mass of BTPE. No other signals are observed, underlining full conversion and stability of the photo-adduct.

Syntheses of Ag-Core Polymer-Shell NPs

Ligand Exchange of BTPE/BTTEG

Commercially available, citrate-capped Ag nanoparticles were centrifuged (30 min x 5000 rpm) and redispersed in the same volume of DMSO. After addition of BTPE and BTTEG in the ratio 1:10 (10 000 eq per Ag nanoparticle), the reaction mixture was incubated overnight at room temperature. Subsequent washing step (40 min x 7000 rpm) removed the free BTPE. To determine the concentration of the resulting Ag-BTPE/BTTEG NPs UV-Vis measurements were performed.

Setup for Light-Triggered Reactions

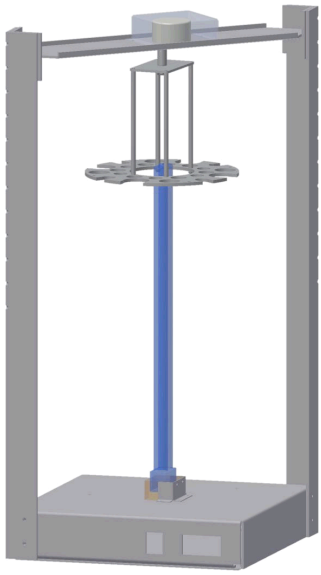

Figure S14. Drawing of the custom-built photoreactor employed in the current study.

The samples to be irradiated were crimped air-tight in headspace vials (20 mm, VWR, Germany) using SBR seals (VWR, Germany) with PTFE inner liner. The photoreactions were performed in a custom-built photoreactor (**Figure S1**) consisting of a metal disk which revolves at a distance of 40-50 mm around a compact low-pressure fluorescent lamp with λ_{max} = 320 nm ± 30 nm (36 W, Arimed B6, Cosmedico GmbH, Germany) (**Figure S2**).

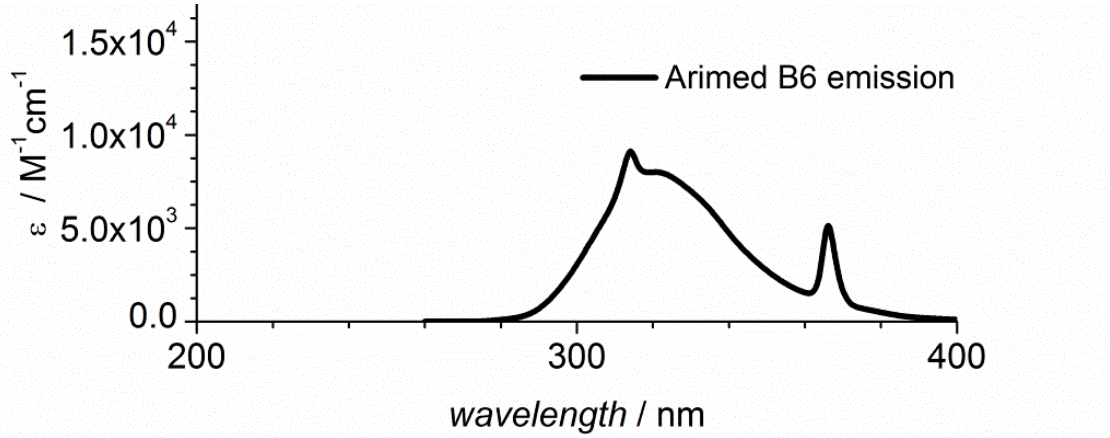

Figure S15. Emission spectrum of the employed compact low-pressure fluorescent lamp (36 W, Arimed B6, λ_{max} = 320 nm).

Photoreaction between Ag-BTPE/BTTEG and PEG-Mal

To Ag-BTPE/BTTEG dispersion (210 fmol, 1 eq) in 400 μL DMSO, PEG-Mal (2.10 nmol, 10000 eq) was added and aliquoted in a headspace vial (Pyrex, diameter 20 mm), which was crimped air-tight using SBR seals with PTFE inner liner. The solution was deoxygenated by purging with nitrogen for 10 min. The flask was subsequently irradiated for 15 min by revolving around a compact low-pressure fluorescent lamp (Arimed B6, Cosmedico GmbH, Stuttgart, Germany) emitting at 320 nm (± 30 nm, 36 W, the emission spectrum of the employed compact low-pressure fluorescent lamp is included in Figure S2) at a distance of 40–50 mm in a custom-built photoreactor (see Figure S1). The excess PEG-Mal was removed by using a 2000 kDa dialysis bag, which allows the polymer (M_n = 1300 g·mol^{-1}) to pass through, while retaining Ag-core PEG-shell NPs.

Photoreaction between Ag-BTPE/BTTEG and poly(CBMA-2)

To Ag-BTPE/BTTEG dispersion (100 fmol, 1 eq) in 400 μL DMSO, poly(CBMA-2) (5.00 nmol, 50000 eq) was added and aliquoted in a headspace vial (Pyrex, diameter 20 mm), which was crimped air-tight using SBR seals with PTFE inner liner. The solution was deoxygenated by purging with nitrogen for 10 min. The flask was subsequently irradiated for 60 min by revolving around a compact low-pressure fluorescent lamp (Arimed B6, Cosmedico GmbH, Stuttgart, Germany) emitting at 320 nm (± 30 nm, 36 W, the emission spectrum of the employed compact low-pressure fluorescent lamp is included in Figure S2) at a distance of 40–50 mm in a custom-built photoreactor (see Figure S1). The excess p(CBMA-2) was removed by centrifugation (3 x).

Zeta Potential

Electrophoretic Light Scattering (ELS) was used to determine the average zeta potential (ζ) of the nanoparticles formed. The measurements were carried out in a Zetasizer NanoZS instrument (Malvern Instruments, UK). The measurements of electrophoretic mobility were converted to ζ-potential through Henry's equation which was calculated using the Smoluchowski approximation.

Table S2. Zeta potential measurement of citrate-capped Ag NPs, BTPE/BTTEG modified Ag NPs and PEG coated Ag NPs.

Nanoparticles	Zeta Potential [mV]	Solvent
Ag-citrate	-35.0 ± 0.3	DMSO
Ag-BTPE/BTTEG	-30.1 ± 0.8	DMSO
Ag-PEG	-29.5 ± 0.7	DMSO
Ag-pCBMA	37.1 ± 2.0	H_2O (pH = 6.40)

Zeta potential values more negative than –30 mV are generally considered to represent sufficient repulsion to ensure the stability of dispersion, as is well known from colloidal science. The citrate-capped Ag NPs had a negative zeta potential due to the negatively charged of the carboxylic acid groups. The ligand exchange of BTPE and BTTEG was accompanied by change of less negative surface charge of Ag-NPs, which was confirmed by reduced negative charge. The zeta potential value remained at approximately at -30 mV after the photoconjugation with PEG-Mal, because the negatively charged hydroxyl groups did not participate in the reaction and the polymer is not charged. However, the photoconjugation of Ag-NPs with zwitterionic pCBMA leads to positive zeta potential due to the positive charge quaternary ammonium cation.

UV-Vis spectroscopy

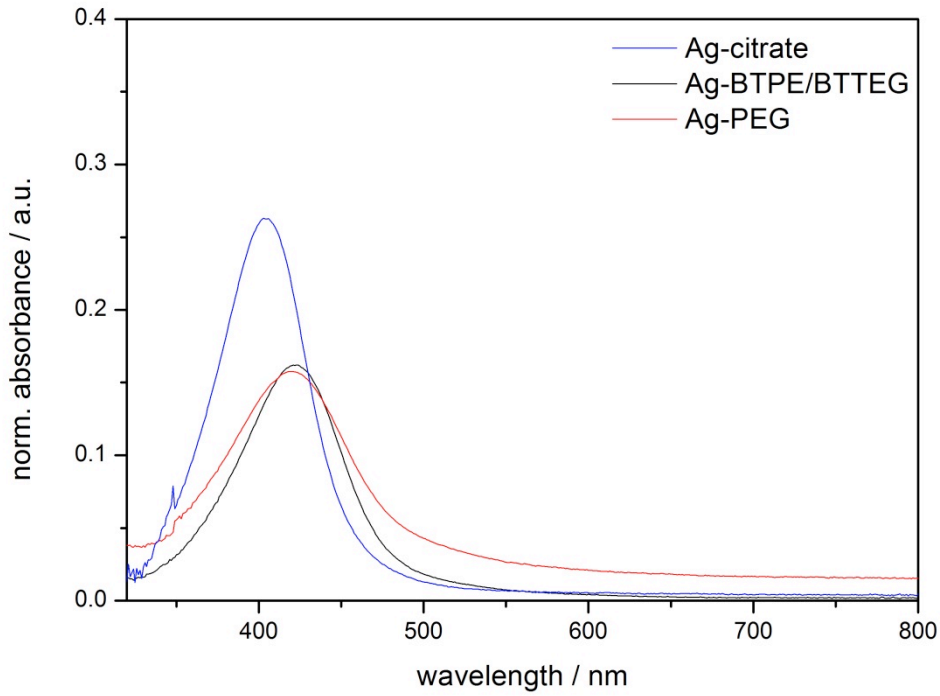

Figure S16. UV-Vis measurement of citrate-capped Ag NPs, BTPE/BTTEG modified Ag NPs and PEG coated Ag NPs.

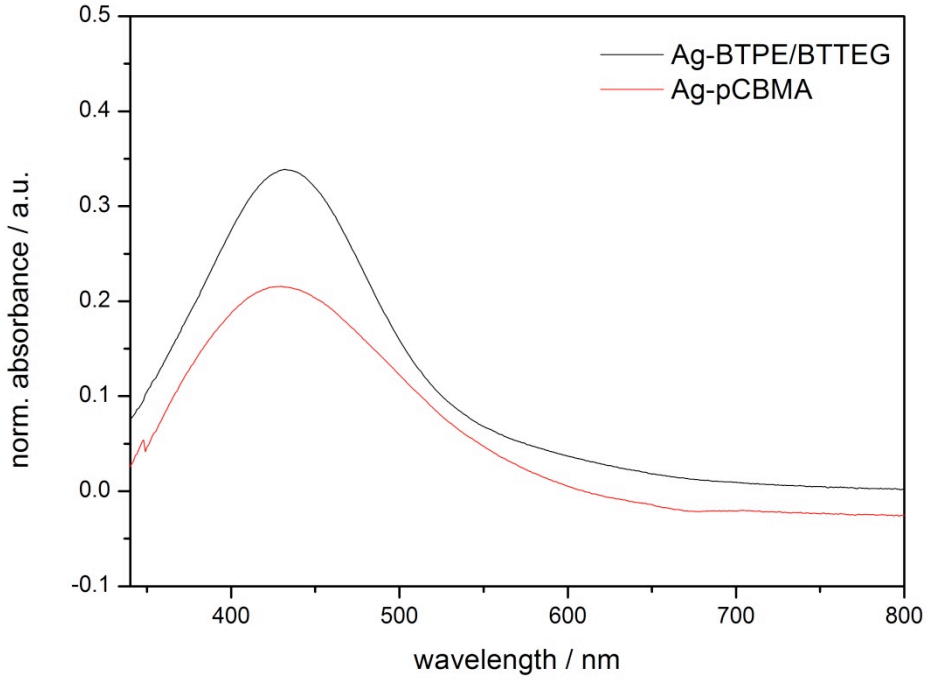

Figure S17. UV-Vis measurement of BTPE/BTTEG modified Ag NPs and pCBMA coated Ag NPs.

UV-Vis measurements were performed for the determination of the Ag NP concentration (ε_{max} = 7.75·10^{9} M^{-1} cm^{-1}; extinction coefficient according to literature)[12] and to proof the stability of the Ag NPs.

TEM Imaging

TEM samples were prepared by putting droplets of sample suspension onto a copper TEM grid covered with a thin amorphous carbon film of less than 3 nm nominal thickness. Subsequently the prepared samples were dried in air at room temperature.

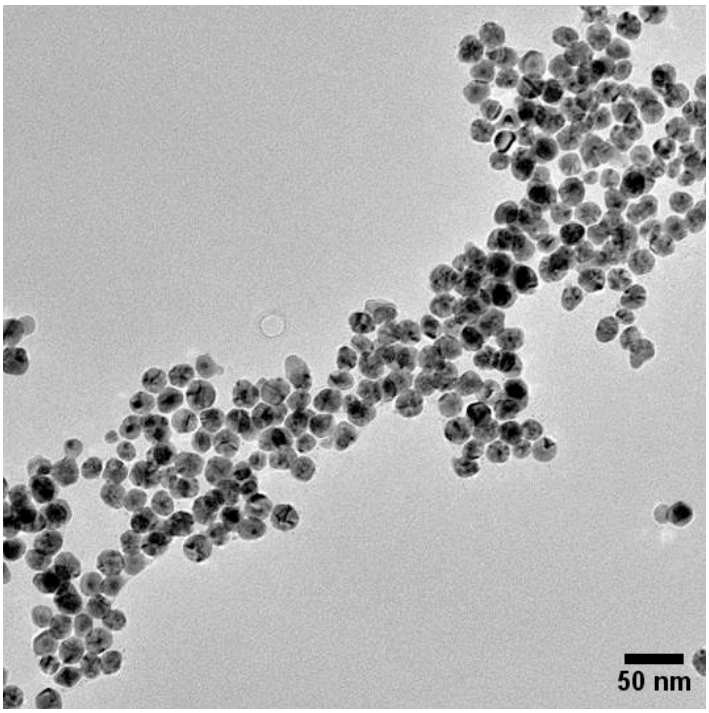

Figure S18. TEM image of commercially available, citrate-capped Ag NPs.

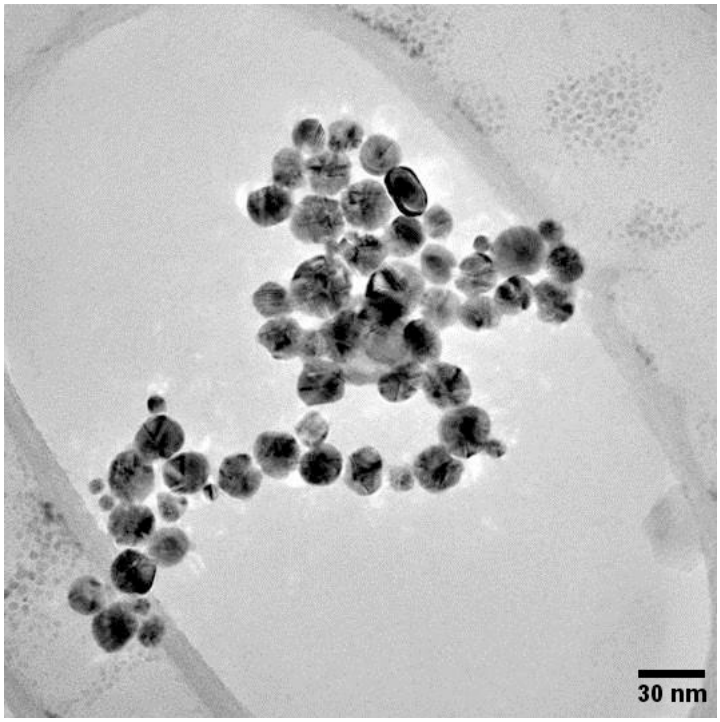

Figure S19. TEM image of Ag NPs after ligand exchange with BTPE and BTTEG.

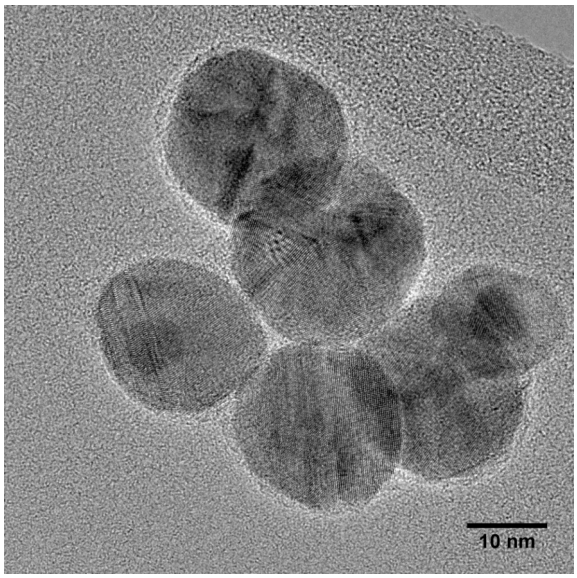

Figure S20. HRTEM image of BTPE modified Ag NPs after the photoreaction with PEG-Mal. The core shell structure of 20 nm Ag and 1-2 nm PEG is visible.

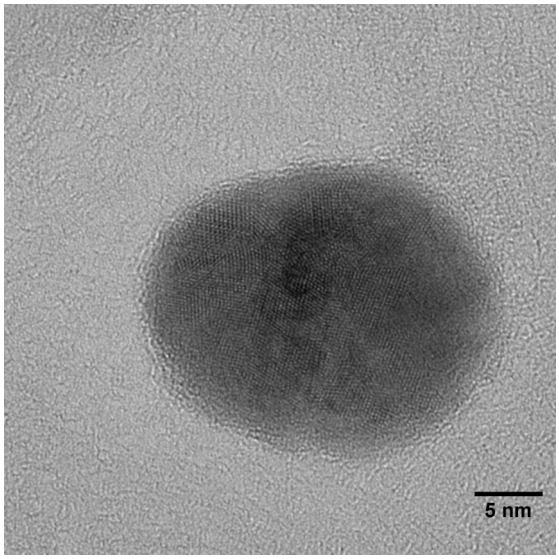

Figure S21. HRTEM image of BTPE modified Ag NPs and PEG-Mal without irradiation as control sample. The polymer is not observable at the surface of the Ag nanoparticles.

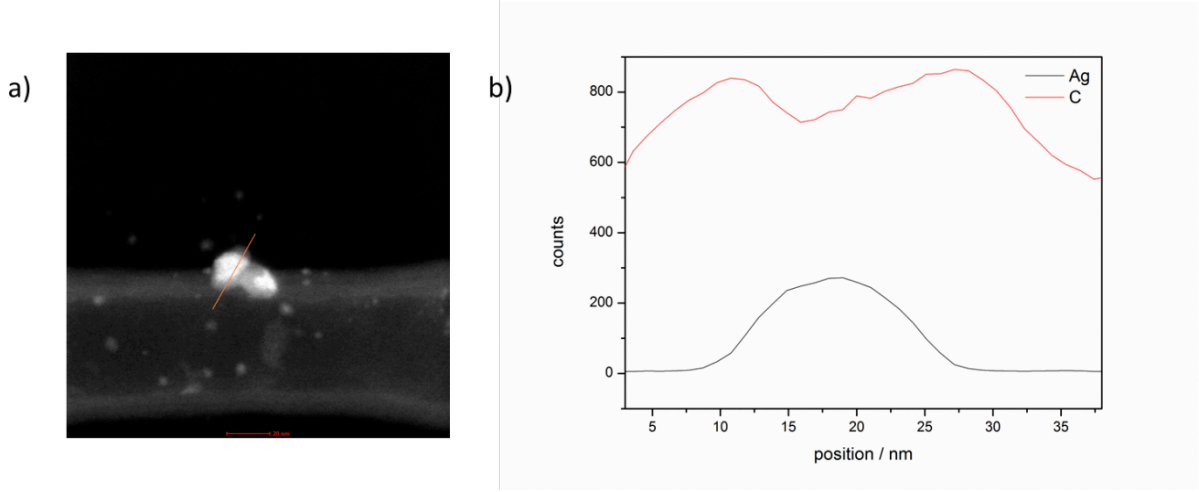

Figure S22. a) High resolution transmission electron microscopy (HRTEM) image shows the Ag NPs with poly(ethylene glycol). The energy-dispersive X-ray spectroscopy (EDXS) line scan follows the orange line. **b)** Carbon and silver peak intensities along the EDXS line scan showing the Ag-PEG core-shell structure. The counts of carbon and silver are plotted against the position. The core is around 20 nm and the shell around 2 nm. The overall slope of the carbon curve was background-corrected to account for slight thickness variation of the carbon support film.

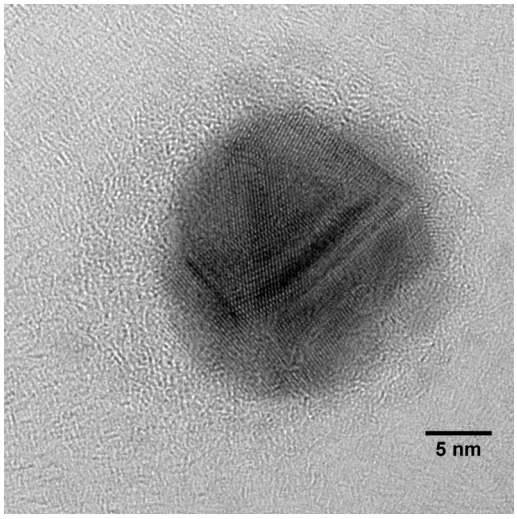

Figure S23. HRTEM image of BTPE modified Ag NPs after the photoreaction with pCBMA-Mal. The core shell structure of 20 nm Ag-core and 4 nm pCBMA-shell is visible.

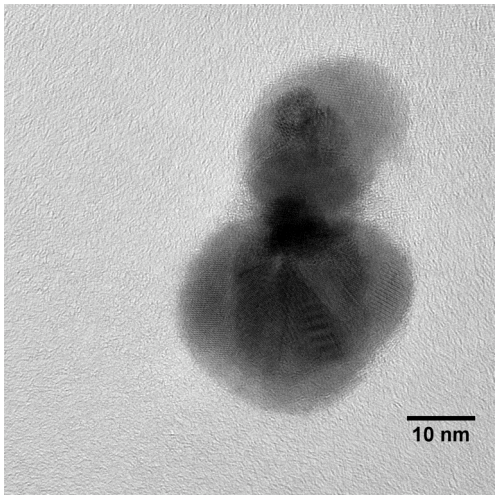

Figure S24. HRTEM image of BTPE modified Ag nanoparticles and pCBMA-Mal without irradiation as control sample. The polymer is not observable at the surface of the Ag NPs.

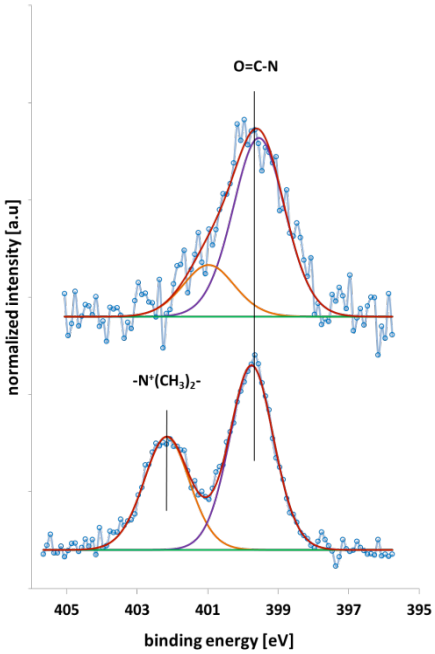

Figure S25. XPS analysis of the BTPE/BTTEG modified AgNPs (top) and pCBMA coated AgNPs shows a new peak at 402.2 eV in N 1s XP spectrum which is assigned to $N^{+}R_4$ bonds, stemming from the quaternary ammonium of the CBMA unit.

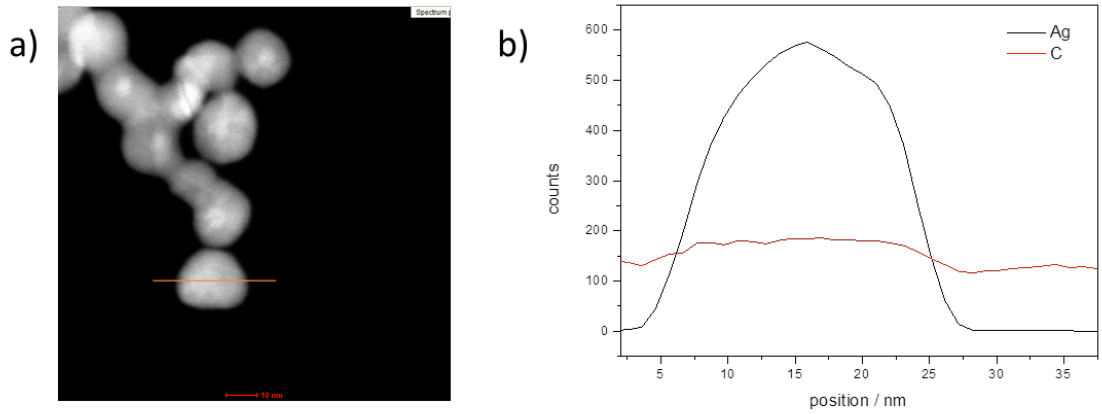

Figure S26. Control sample of BTPE modified Ag NPs and PEG-Mal without irradiation after one washing step. **a)** High resolution transmission electron microscopy (HRTEM) image shows the Ag NPs. The energy-dispersive X-ray spectroscopy (EDXS) line scan follows the orange line. **b)** The counts of carbon and silver are plotted against the position. Carbon and silver peak intensities along the EDXS line scan showing no higher amount of carbon on the surface of the Ag NP. The core is around 20 nm and no shell is observable. The counts of carbon are caused by the carbon support film.

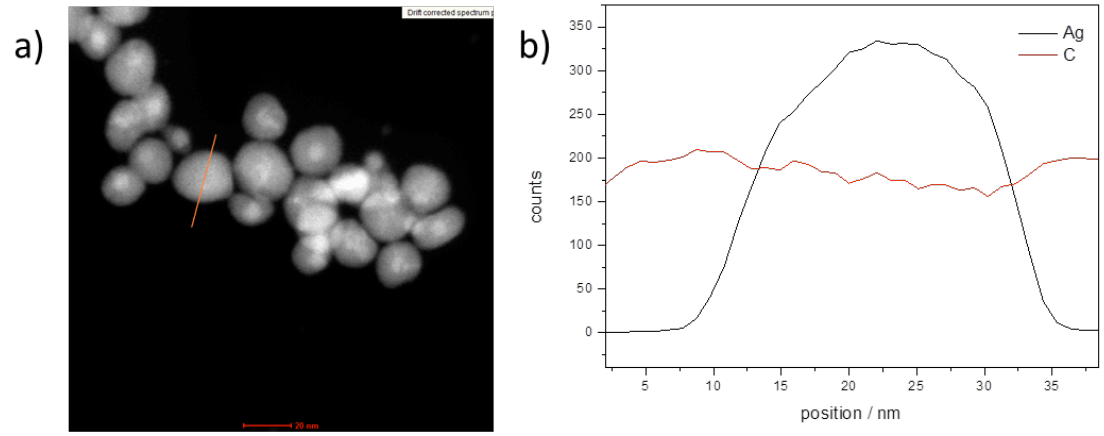

Figure S27. Control sample of BTPE modified Ag NPs and pCBMA-Mal without irradiation after one washing step. **a)** High resolution transmission electron microscopy (HRTEM) image shows the Ag NPs. The energy-dispersive X-ray spectroscopy (EDXS) line scan follows the orange line. **b)** The counts of carbon and silver are plotted against the position. Carbon and silver peak intensities along the EDXS line scan showing no higher amount of carbon on the surface of the Ag NP. The core is around 20 nm and no shell is observable. The counts of carbon are caused by the carbon support film.

References

1. T. Pauloehrl, G. Delaittre, V. Winkler, A. Welle, M. Bruns, H. G. Borner, A. M. Greiner, M. Bastmeyer and C. Barner-Kowollik, *Angew Chem Int Ed Engl*, 2012, **51**, 1071-1074.
2. M. Glassner, K. K. Oehlenschlaeger, T. Gruendling and C. Barner-Kowollik, *Macromolecules*, 2011, **44**, 4681-4689.
3. K. L. Parry, A. G. Shard, R. D. Short, R. G. White, J. D. Whittle and A. Wright, *Surf. Interface Anal.*, 2006, **38**, 1497-1504.
4. S. Tanuma, C. J. Powell and D. R. Penn, *Surf. Interface Anal.*, 1994, **21**, 165-176.
5. J. H. Scofield, *J. Electron Spectrosc. Relat. Phenom.*, 1976, **8**, 129-137.
6. Y. Jung, J. M. Lee, J. W. Kim, J. Yoon, H. Cho and B. H. Chung, *Anal. Chem.*, 2009, **81**, 936-942.
7. A. V. Delgado, E. Gonzalez-Caballero, R. J. Hunter, L. K. Koopal and J. Lyklema, *Pure Appl. Chem.*, 2005, **77**, 1753-1805.
8. G. Mantovani, F. Lecolley, L. Tao, D. M. Haddleton, J. Clerx, J. J. Cornelissen and K. Velonia, *J. Am. Chem. Soc.*, 2005, **127**, 2966-2973.
9. H. Lee, S. M. Dellatore, W. M. Miller and P. B. Messersmith, *Science*, 2007, **318**, 426-430.
10. C. Rodriguez-Emmenegger, E. Brynda, T. Riedel, M. Houska, V. Šubr, A. Bologna Alles, E. Hasan, J. E. Gautrot and W. T. S. Huck, *Macromol. Rapid Commun.*, 2011, **32**, 952–957.
11. C. Rodriguez-Emmenegger, E. Hasan, O. Pop-Georgievski, M. Houska, E. Brynda and A. Bologna Alles, *Macromol. Biosci.*, 2011, **12**, 525-532.
12. J. R. Navarro and M. H. Werts, *Analyst*, 2013, **138**, 583-592.